

## Development of a New Armor Steel and its Ballistic Performance

Ş. Hakan Atapek

Kocaeli University, Kocaeli, 41380- Turkey

Email: [hatapek@kocaeli.edu.tr](mailto:hatapek@kocaeli.edu.tr)

### ABSTRACT

In this study, a boron added armor steel was developed according to standard rolled homogenous armor steel, MIL-A-12560, and metallographic-fractographic examinations were carried out to understand its deformation characteristics and perforation mode after interaction with a 7.62 mm armor piercing projectile. The microstructure of the developed steel was characterized by light and scanning electron microscope to evaluate its matrix after application of several heat treatments consisting of austenization, quenching and tempering. The mechanical properties of the developed steel were determined by tensile test at room temperature and notched impact test at -40 °C. The ballistic performance of developed steel was determined by its V50 ballistic protection limit according to MIL-STD-662F standard and it was found to be higher than that of MIL-A-12560 steel. After perforation deformation induced adiabatic shear bands, that have an important role on the crack nucleation, were observed close to the penetration in the etched steel and perforation occurred by typical ductile hole enlargement with certain radial flows.

**Keywords:** Armor steel, dynamic loading, adiabatic shear band, perforation

### 1. INTRODUCTION

Alloying and processing metallurgy are very important in the development of armor steels<sup>1</sup>. An armor steel should have properties like (a) high resistance to perforation and ballistic impacts, (b) possible fabricability, (c) adequate fatigue and wear resistance under service conditions<sup>2</sup>. Sangoy<sup>3</sup>, *et al.* reported that high hardness of a given armor steel directly determines the ballistic performance and perforation mode. However, there is no basic correlation between hardness and resistance to perforation, as measured by the protection ballistic limit. In order to obtain high hardness values, studies on alloying design and heat treatment conditions are very popular to improve the ballistic performance of the steels<sup>4-7</sup>. On the other hand, toughness is the another critical property for a given armor material under a dynamic attack of projectiles having high kinetic energies<sup>8</sup>. It is generally considered that armor steels having high toughness will be very useful to resist ballistic impacts without being fractured. As it is well known, alloying and also heat treatments affect the toughness of the materials. Fabrication includes many operations such as cutting, welding machining and forming. Sangoy<sup>3</sup>, *et al.* summarized the fabrication operations (thermal cutting, welding, machining etc.) and required metallurgical properties for the armor steels. Low carbon equivalent, limited segregation, low hydrogen content, low residual stress, high ductility are the main requirements under mentioned fabrication operations. Armor steels must be weldable and fatigue behaviour of these materials must be higher under cyclic stresses. Weld quality directly determines the whole mechanical properties of the armor steel<sup>9,10</sup>.

Conventional armor steels are quenched and tempered alloy steels having martensitic/bainitic or tempered martensitic/bainitic matrix<sup>11</sup>. Ade<sup>10</sup> compared the armor steels as class I, class II, high hardness and cast steels at 1 inch thickness. These steels have different alloy compositions and heat treatment conditions, therefore, they have different matrices and mechanical properties such as strength, hardness and toughness at -40 °C. Class I (MIL-A-12560) is the standard armor steel having 34-40 HRC hardness and is used in vehicle applications. Class II has the same chemical composition as class I, but it is heat treated at higher tempering temperatures. Its hardness changes in the range of 29-34 HRC. High hardness type is used when the high penetration resistance is required. Cast armor steels, on the other hand, are commonly used in complex shape applications<sup>10</sup>.

The working principle of a typical armor material depends on the reality of stopping the attack by the sharp tip of -steel or other heavy metal-based penetrator, with its high hardness. In order to understand the behaviour of an armor steel to a given armor penetrator, the concepts such as shock, deformation and fracture during penetration and perforation must be known. This is the reason why the study of perforation mechanisms is required. As hardness and strength of armor steel increase, penetration resistance will also increase. The performance is directly related to fracture mode that is effective at specific levels of hardness<sup>12,13</sup>.

In this study, a quenched followed by tempered steel was developed as an armor material. The steel was investigated by metallographic and fractographic examinations before and after ballistic shots. Alloying design, heat treatment applications

and the microstructural characterization were emphasized in the first step of the study. In the second step, perforation mode and fracture behaviour of the steel were examined.

## 2. EXPERIMENTAL STUDY

### 2.1 Material and Methods

The alloy composition used in the experimental study is given in Table 1. Chromium and molybdenum have been selected for precipitation hardening and niobium, vanadium, titanium have been added as microalloying elements. Cobalt is chosen to increase the toughness of the matrix. The amount of carbon has been adjusted to a low level for a good weldability. Boron has been added to promote on one side the martensitic/bainitic transformation, on the other side precipitation of borides/carborides<sup>14</sup>.

**Table 1. The chemical composition (wt %) of the experimental steel**

C	Mn	Si	Ni	Co	Cr	Mo
0.23	0.19	0.19	0.04	2.35	1.40	0.50
Nb	V	Ti	B	P	S	Fe
0.08	0.08	0.002	0.002	0.01	0.01	balance

An armor steel, used as an armor material, is produced primarily by pure casting as well as casting and rolling. Steel has been cast with an AEG medium frequency furnace in 7<sup>th</sup> Maintenance Center of Turkish Land Forces Command at Istanbul. The steel has solidified in a dendritic form due to the solidification rates generally practiced in the ingot metallurgy of the Maintenance Center. Prior to casting, the alloy is kept for approximately 200 s at a temperature range of 60 °C - 100 °C above the calculated liquid temperature. A minimum cooling rate of 1 K/s is maintained until the melt solidified completely. After casting, homogenization annealing was performed on the slab at 1230 °C and then the slab was rolled at 1200 °C in 11 passes to get a plate 12.7 mm in thickness. The plate was deformed according to the standard operating procedures of Erdemir Co. (Zonguldak-Turkey).

Heat treatment is one of the most important concepts for the improvement of mechanical properties of a given metal or alloy system. Table 2 shows the heat treatment conditions of the experimental steel. The austenization, quenching and finally tempering heat treatments were performed on the steel plate as commercial applications. Table 3 shows the mechanical

**Table 2. The heat treatment conditions of the experimental steel**

Austenization	Quenching	Tempering
1000 °C, 45 min.	Oil quenching	600 °C, 45 min.

**Table 3. The mechanical properties of tempered martensitic steel and standard rolled homogenous armor steel (MIL-A-12560)**

Materials	Hardness (HRC)	Tensile Strength (MPa)	Elongation (%)	Impact Toughness*(J/mm <sup>2</sup> )
Standard (MIL-A-12560)	34-40**	1250	≥ 10	30-40**
Experimental	38	1250	11.3	10.7

(\*) Test temperature : -40°C, (\*\*) Hardness and impact toughness depend on applied heat treatment (Sangoy, 1988; Ade, 1991).

properties of the experimental steel in comparison with the MIL-A-12560 standard armor steel. Tensile test and notched impact test were performed according to TS 138 EN 10002-1 [ISO 6892 (ENQ)] and TS EN 10045-1 [ISO 148:1983], respectively. The mechanical properties are very important parameters to understand the performance of materials against any external effect during service conditions. As seen from Table 3, hardness, strength and elongation values of the experimental steel are very close to that of the standard. A high impact toughness value is inevitable for MIL-A-12560 which is a very clean steel.

### 2.2 Ballistic Shots

Steel plate of 300 nm x 1000 mm in size were prepared for the ballistic test and the ballistic test was performed at the laboratories of FNSS Defence Systems Co. (Ankara-Turkey). The ballistic performance of developed steel was determined by its V50 ballistic protection limit according to MIL-STD-662F standard. Shot was done with 7.62 AP M2 type projectile at 0°, the distance of shot is 30 m and distance between target and witness plate was 15.24 cm.

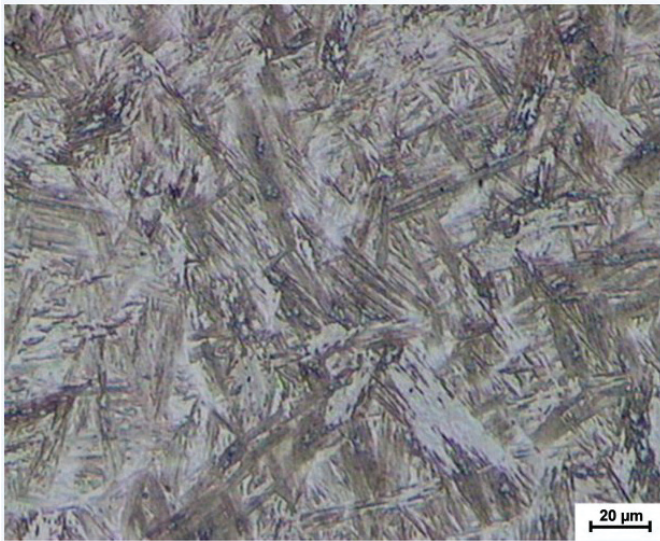
### 2.3 Metallographical Sample Preparation

All samples for the microstructural characterization were prepared by grinding with 320, 600, and 1000 mesh size SiC abrasives respectively and then ground surfaces were polished with 3 µm diamond solution. Etching was required to determine the phases within the matrix, and in this study etching was carried out with initial (% 3 HNO<sub>3</sub>) to characterize the microstructure.

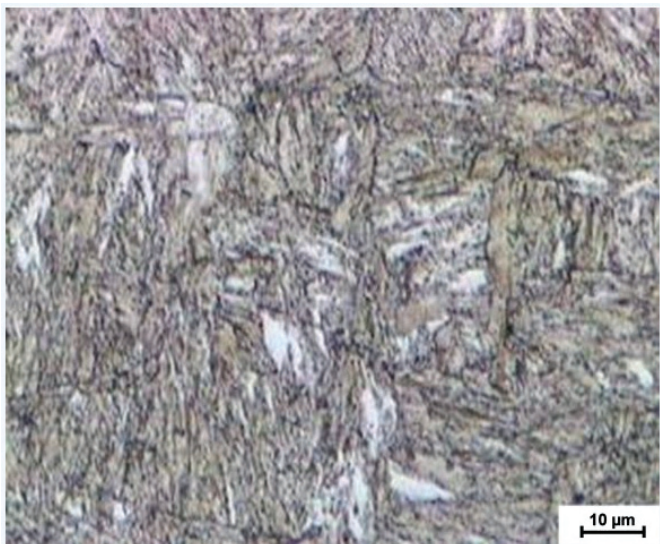
## 3. RESULTS AND DISCUSSIONS

### 3.1 Microstructural Characterization before Ballistic Shot

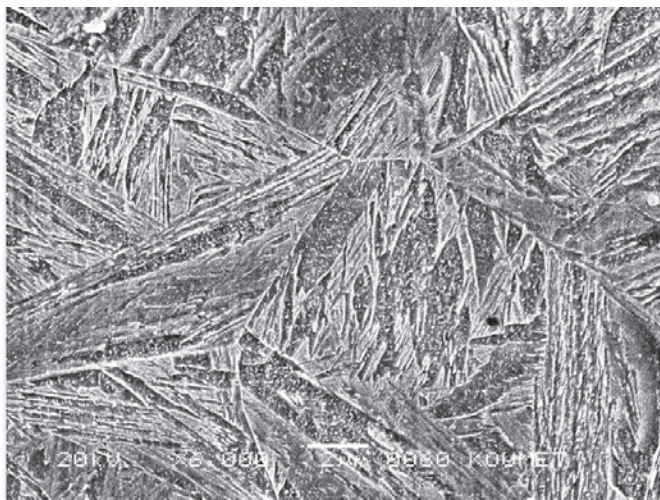
Figure 1(a) shows an example of the microstructure after quenching. As seen, steel has a matrix consisting of lath-type martensite due to rapid cooling. Figures 1(b) and (c) represent tempered martensitic microstructure of the experimental steel. This kind of microstructure includes a ferritic matrix and intensively dispersed precipitates at the interfaces of ferrite laths. These precipitates are mainly cementite but secondary carbides can also take place in the matrix due to tempering at 500 °C - 600 °C<sup>15,16</sup>. The secondary carbides in the matrix increase the hardness and strength of the steel depending on the density per unit volume and the interaction with dislocations in addition to having coherent or semi-coherent interfaces<sup>17</sup>. Transmission electron microscopes (TEM) are very useful to determine the size, shape and distribution of these particles. The content of these particles can be determined using scanning transmission electron microscope attached energy dispersive x-ray spectrometer (STEM/EDS) or atom probe field ion microscope (APFIM)<sup>18-22</sup>.



(a)



(b)



(c)

**Figure 1.** The microstructures of the experimental steel (a) as quenched, (b) as tempered and (c) scanning electron microscope micrograph of tempered martensitic matrix.

### 3.2 Ballistic Performance

The ballistic test was performed by 7.62 mm AP projectile at 0° to determine V50 ballistic limit according to MIL-STD-662F. V50 ballistic limit is the most common method for assessing the ballistic performance of lightweight armor materials. Accordingly, the final state of a witness plate placed behind the armor panel determines the experimental outcome of the ballistic test. Complete penetration (CP) takes place when the witness plate is completely perforated by the projectile or plate spall. Partial penetration (PP) occurs if no perforation is observed through the witness plate<sup>23</sup>. In the ballistic test of the experimental steel, 12 shots are made from 30 meters to target and V50 ballistic limit is calculated as the arithmetical mean of lower and higher values of PP and CP after macro examinations on perforated regions. The first two shots were for calibration purpose. All shot data are given in Table 4.

**Table 4.** Shot conditions and results for the ballistic test

Shot number*	Output velocity, m/s	Striking velocity, m/s	Evaluation**
01	732	730	PP
02	753	751	PP
03	777	775	<i>PP</i>
04	775	772	PP
05	812	809	CP
06	783	780	<i>CP</i>
07	771	768	PP
08	791	788	CP
09	809	807	CP
10	753	751	PP
11	767	764	PP
12	779	777	<i>PP</i>

V50 (standard) : 750 m/s

V50 (experimental) : 780 m/s

\* The first two shots were for calibration purpose.

\*\* The values used for calculation of ballistic limit are written in bold and italic

Figure 2 shows the comparison of the V50 ballistic limits of the standard and experimental steels. As seen, the experimental steel has a higher V50 ballistic limit than the standard.

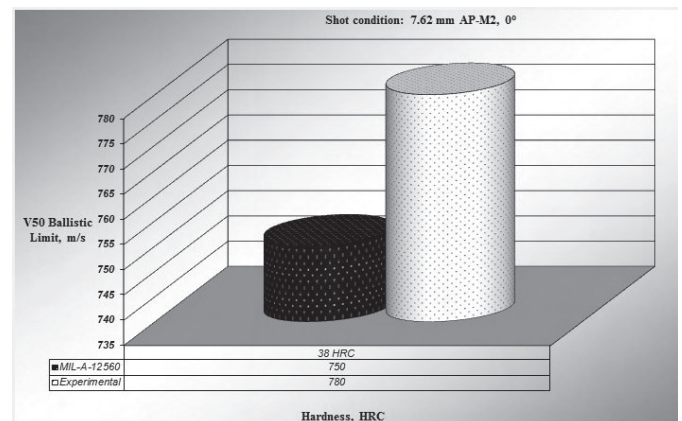


**Figure 2.** A comparison of V50 ballistic limit as a function of hardness for MIL-A-12560 and experimental steel.

### 3.3 Deformation and Failure

There are several perforation modes such as hole enlargement, plugging, discing, spalling and radial fracture. Hole enlargement by plastic deformation occurs on low resistance, ductile material targets which are perforated by undeformable ogival-head projectiles upsetting the metal along the craterization path, thus causing metal radial flow and hole formation by ductile deformation. Plugging is embodied by the ejection from the back of the target of a plug having a diameter about equal to that of projectile. On the other hand, discing is embodied either by small fragments being formed or a disc being separated from the back of the target then acting as a secondary projectile. Adiabatic shear bands have an important role on the formation of plugging and discing type perforation modes under dynamic loading conditions. Spalling is due to the failure of a disc from the back of the target under the effect of

tensile stresses due to reflections of the shock wave induced by the impact. And finally, radial fracture occurs in brittle targets and is initiated around the point of impact of projectile<sup>3</sup>.

A light microscope image of experimental steel after perforation is given in Fig. 3(a). A crater type dimple may occur by the interaction of projectile with the target material. At first interaction of projectile with the target, it is possible to form brittle rupture without any plastic deformation due to high impact energy/loading and a crater forms (Fig. 3(b)). Figure 3(c) is a good example which indicates the formation of soft perforation and it refers to hole enlargement by excellent plastic deformation. Radial flow by plastic deformation is illustrated in Fig. 3(d).

A typical adiabatic shear band formed in the matrix of the experimental steel due to high strain by impact loading of the projectile is clearly seen in Fig. 4. In high strain rates, the

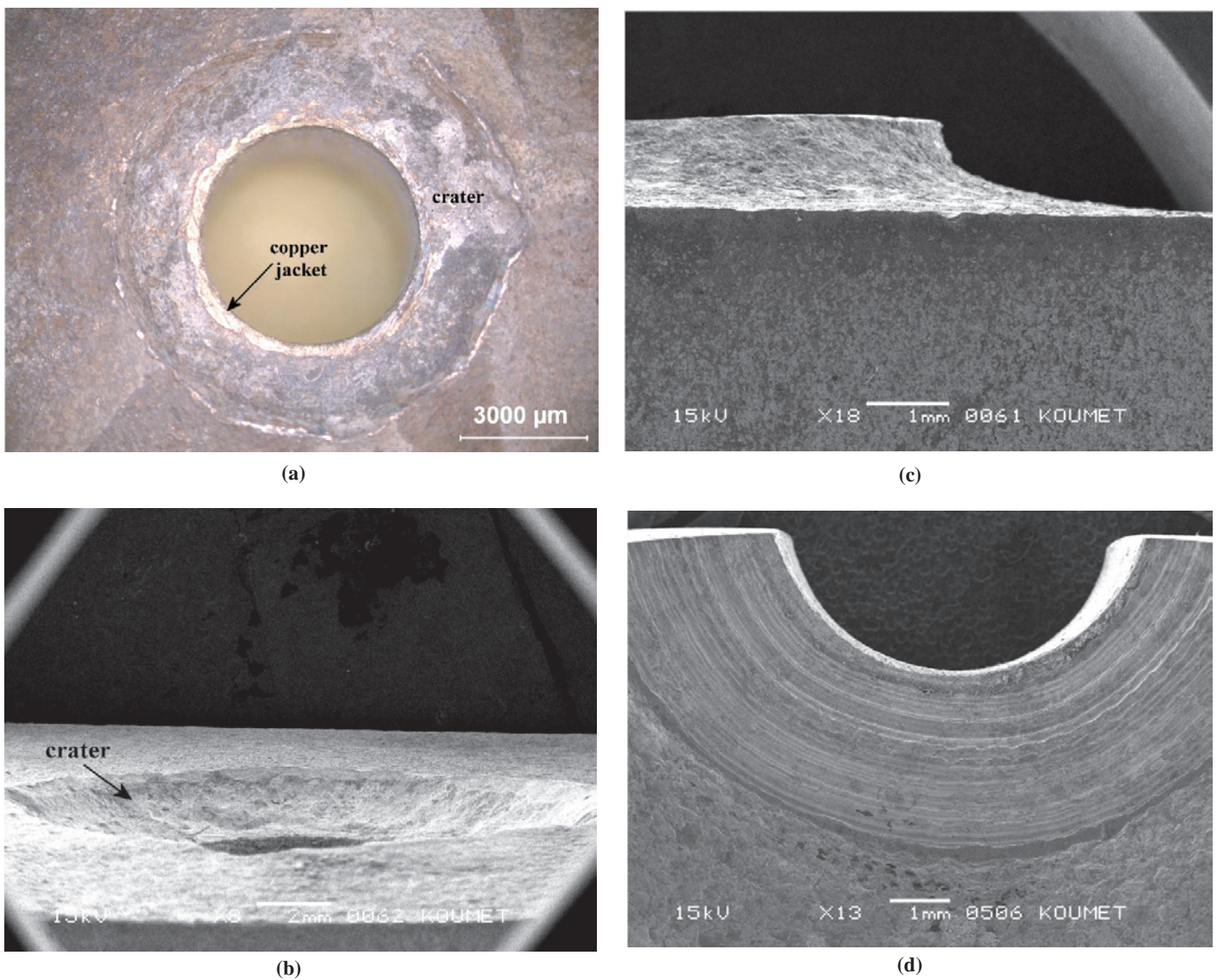


**Figure 3.** (a) A light microscope image of the perforated zone of experimental steel showing copper jacket of projectile and crater due to interaction of projectile with the target steel, (b) a dimple formation indicating the craterization, (c) a simple example of plastic deformation in the experimental steel due to elongation of the material from back of target along the direction of penetration, (d) radial flow tracks formed by penetration of projectile and high plastic deformation of matrix.

materials exhibit local deformation known as adiabatic shear. Adiabatic shear bands form as a result of a thermo-mechanical instability due to the presence of a local inhomogeneity, including local deformation and heating. If the thermal conductivity of the material is not sufficient to conduct the generated heat away, deformation becomes unstable and is localized on surfaces of very small thickness. This temperature rise softens the localized area, accelerates plastic instability and induces microstructural evolutions<sup>24</sup>. This situation is compatible to the interaction of a projectile with a steel target. High temperatures can form because of high friction of the projectile during penetration. There have been many studies on adiabatic shear bands, but each study has different approaches and theoretical background such as dynamic recovery, dynamic recrystallization and phase transformation<sup>25-31</sup>. In microscopic examination, adiabatic shear bands appear as narrow bands in which cracks can propagate, indicating catastrophic failure of the material. Shear bands in different metals could be broadly classified as either ‘transformed’ or ‘deformed’ on the basis of their appearance in metallographic section. Deformed bands are characterized by a very high shear strain in a very thin zone of deformation. Inside the band the grains are highly distorted, but there is no evident change in the structure of the material. In transformed bands, a crystallographic phase change occurs. In steels, they are often called ‘white bands’ because of their appearance after etching and are quite different from the matrix<sup>32</sup>. An example for this appearance is illustrated in Fig. 4(a). The formation of adiabatic shear band results in several perforation modes (e.g. plugging and discing type fracture) in armor steel<sup>3</sup>. Figure 4(b) shows the degenerated matrix due to impact loading and rapid deformation. This region has smaller grains than the original matrix because of strong deformation and recrystallization. As mentioned before, adiabatic shear bands are very effective on the formation of cracks in the matrix under dynamic loading. Bassim<sup>33</sup>, *et al.* reported for AISI 4340 steel that cracks are initiated in adiabatic shear band leading to specimen fragmentation along the shear bands. Five stages have been identified for the process of crack initiation and propagation inside ASBs in martensitic high-strength, low alloy steels:

- Formation of microvoids inside the shear bands,
- Coalescence of these microvoids to form void-clusters which elongate parallel to the shear bands,
- Initiation of microcracks from the ends of the void clusters,
- Lengthwise growth and interconnection of adjacent microcracks,
- Crack growth and propagation to failure<sup>33</sup>.

Atapek studied on the formation of adiabatic shear bands in a tempered steel under dynamic loading and their damage effects and both microstructural and fractographic characterization indicated the role of deformed and transformed adiabatic shear bands as a crack promoter<sup>34</sup>. An example of this effect is represented in Fig. 4(c). This figure indicates a crack formation at the tip of adiabatic shear band.

#### 4. CONCLUSIONS

In this study, the microstructure, mechanical and ballistic

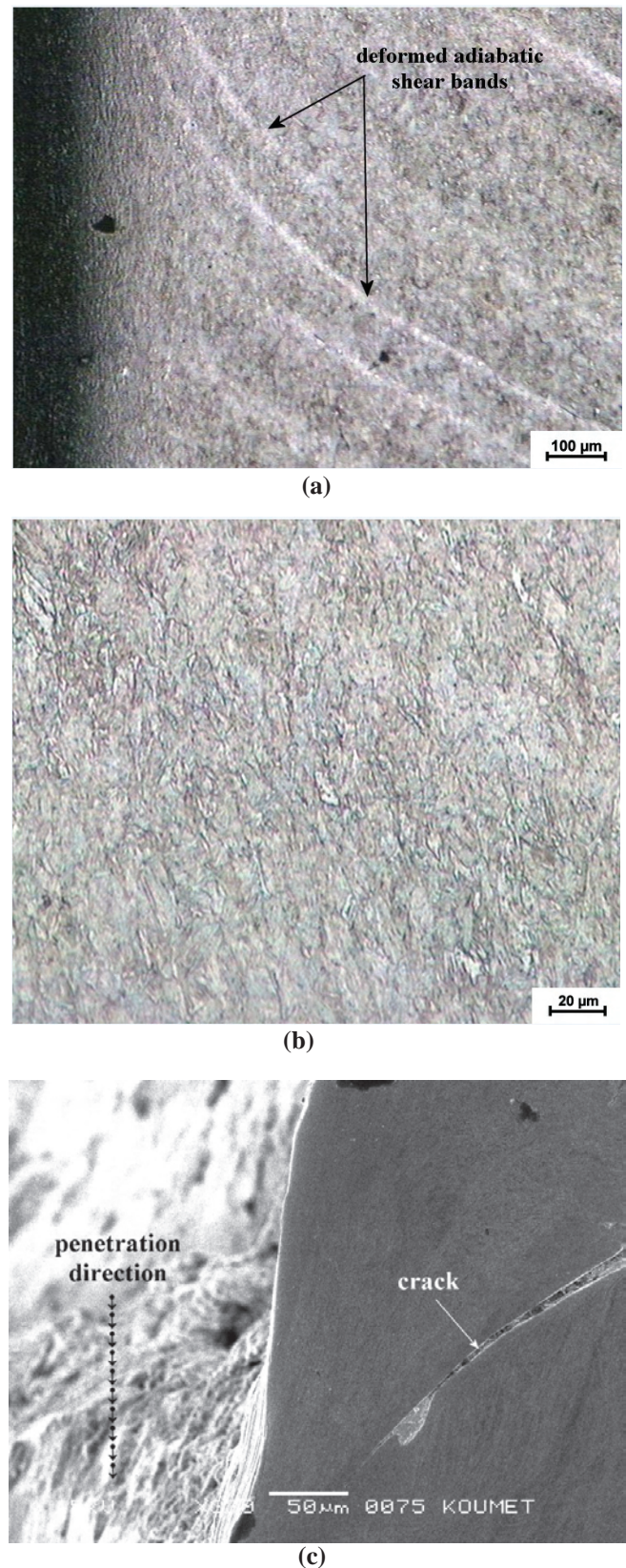


Figure 4. (a) Deformed adiabatic shear bands formed in the matrix of the experimental steel due to high strain by impact loading of the projectile, (b) the matrix consisting of smaller grains than the original matrix because of strong deformation and recrystallization, and (c) a crack formation at the tip of adiabatic shear band.

performance of a tempered martensitic steel were investigated in comparison with MIL-A-12560 armor steel and the following results were obtained;

- (1) A new alloy design and a conventional heat treatment series including austenization, quenching and tempering were selected to evaluate the steel matrix as a candidate for armor steel. After applying heat treatments, a tempered martensitic matrix having a hardness value of 38 HRC was obtained.
- (2) Standard tensile and impact tests were performed on the experimental steel to determine mechanical properties such as tensile strength, elongation (%) and impact toughness. All mechanical properties are optimal for the experimental steel compared to the standard armor steel MIL-A-12560.
- (3) The ballistic test was performed by 7.62 AP at 0° to determine V50 ballistic limit according to MIL-STD-662F. Complete and partial penetration (CP and PP) values after shots were used to determine V50 ballistic limit. After the ballistic test, the experimental steel displayed a higher V50 ballistic limit than the standard MIL-A-12560 armor steel. Deformation and failure characteristics of the experimental steel after ballistic test were evaluated by examining the sample using light and scanning electron microscope. Typical deformed adiabatic shear band was observed as white bands close to the direction of penetration of the sample. Degenerated matrix in the perforated zone behaves like a strain hardened material due to impact loading and rapid deformation. This region has a smaller grain size than the original matrix because of strong deformation and recrystallization. The effect of adiabatic shear band on the formation of crack nucleation and propagation was illustrated. This formation will easily cause the failure of the target material.
- (4) The experimental steel exhibits a hole enlargement by high plastic deformation under dynamic loading. Radial flow tracks formed by penetration of projectile indicate high plastic deformation of matrix under dynamic loading.

## REFERENCES

1. Crouch, I.G. Metallic armour- from cast aluminium alloys to high strength steels. *Mater. Forums*, 1988, **12**, 31-37.
2. Atapek, Ş.H. Development of a boron added armor steel along the principles of physical metallurgy and evaluation of its ballistic performance. Kocaeli University, Kocaeli, Turkey, 2011. PhD Thesis.
3. Sangoy, L.; Meunier, Y. & Pont, G. Steels for ballistic protection. *Isr. J. Technol.*, 1988, **24**(1-2), 319-326.
4. Karagöz, Ş.; Atapek, Ş.H. & Yılmaz, A. Microstructural and fractographical studies on quenched and tempered armor steels. *Mater. Test.*, 2010, **52**(5), 316-322.
5. Jena, P. K.; Mishra, B.; RameshBabu, M.; Babu, A.; Singh, A. K.; SivaKumar, K. & Bhat, T. B. Effect of heat treatment on mechanical and ballistic properties of a high strength armour steel. *Int. J. Impact Eng.*, 2010, **37**(3), 242-249.
6. Jena, P.K.; Kumar, K.S.; Krishna, V.R.; Singh A.K. & Bhat, T.B. Studies on the role of microstructure on performance of a high strength armour steel. *Eng. Fail. Anal.*, 2008, **15**(8), 1088-1096.
7. Maweja, K. & Stumpf, W. The design of advanced performance high strength low-carbon martensitic armour steels : Microstructural considerations. *Mater. Sci. Eng. A*, 2008, **480**(1-2), 160-166.
8. Atapek, Ş.H. & Karagöz, Ş. Ballistic impact behaviour of a tempered bainitic steel against 7.62 mm armor piercing projectile. *Def. Sci. J.*, 2011, **61**(1), 80-86.
9. Akca, C. & Karaaslan, A. Weldability of class 2 armor steel using gas tungsten arc welding. *Arch. Mater. Sci. Eng.*, 2008, **34**(2), 110-112.
10. Ade, F. Ballistic qualification of armor steel weldments. *Weld. J.*, 1991, **70**(9), 53-58.
11. Maweja, K.; Stumpf, W. & Van der Berg, N. Characteristic of martensite as a function of the Ms temperature in low-carbon armour steel plates. *Mater. Sci. Eng. A*, 2009, **519**(1-2), 121-127.
12. Demir, T.; Übeyli, M. & Yıldırım, R.O. Investigation on the ballistic impact behaviour of various alloys against 7.62 mm armor piercing projectile. *Mater. Design*, 2008, **29**(10), 2009-2016.
13. Dikshit, S.N. Influence of hardness on perforation velocity in steel armour plates. *Def. Sci. J.*, 2000, **50**(1), 95-99.
14. Werner, Dietrich H. Bor und borlegierte staehe. 1. Auflage, Verlag Stahl Eisen, Deutschland, 1990, pp. 35-38. (Dutch)
15. Honeycombe, R.W.K. Steels-microstructure and properties, Metallurgy and Materials Science Series, Edward Arnold, London, UK, 1981, pp. 125-135.
16. Matsubara, H.; Osuka, T.; Kozasu, I. & Tsukada, K. Optimization of metallurgical factors for production of high strength, high toughness steel plate by controlled rolling. *Transaction ISIJ*, 1972, **12**(6), 435-443.
17. Stiller, K.; Karagöz, Ş.; Andren, H.O. & Fischmeister, H. Secondary hardening in high speed steels. *J. Phys. Colloques*, 1992, **48**(C6), 405-410.
18. Gingell, A.D.B.; Bhadeshia, H.K.D.H.; Jones, D.G. & Mawella, K.J.A. Carbide precipitation in some secondary hardened steels. *J. Mater. Sci.*, 1997, **32**(18), 4815-4820.
19. Fischmeister, H.; Liem, I. & Karagöz, Ş. Carbide analysis in high speed steels with the analytical scanning transmission electron microscope (STEM-EDS). *Prakt. Metallogr.*, 1988, **25**(12), 568-577.
20. Fischmeister, H.; Karagöz, Ş. & Andren, H.O. An atome probe study of secondary hardening in high speed steels. *Acta Metall.*, 1988, **36**(4), 817-825.
21. Andren, H. O.; Karagöz, Ş.; Cai Guang-Jun; Lundin, L. & Fischmeister, H. F. Carbide precipitation in chromium steels. *Surf. Sci.*, 1991, **246**(1-3), 246-251.
22. Karagöz, Ş.; Fischmeister, H.F.; Andren, H.O. & Cai-Guang Jun. Microstructural changes during overtempering of high speed tool steels. *Metall. Trans. A*, 1992, **23**(6), 1631-1640.
23. Craig, B.D.; Lane, R.A. & Babcock, W.G. Materials for blast and penetration resistance. *AMPTIAC Quartely*, 2004, **6**(4), 39-45.
24. Hwang, B.; Lee, S.; Kim, Y.C.; Kim, N.J. & Shin, D.H. Microstructural development of adiabatic shear bands in

- ultra-fine grained low-carbon steels fabricated by equal channel angular pressing. *Mater. Sci. Eng. A*, 2006, **441**(1-2), 308-320.
25. Timoty, S.P. & Hutching, I.M. The structure of adiabatic shear bands in a titanium alloy. *Acta Metall.*, 1985, **33**(4), 667-676.
  26. Zhou, J.S.; Zhen, L.; Cui, Y.X. & Yang, D.Z. Transformed shearing bands in strongly impact loaded 30CrMnSiA steel. *J. Mater. Sci. Lett.*, 1998, **17**(5), 391-393.
  27. Murr, L.E. & Esquivel, E.V. Observations of common microstructural issues associated with dynamic deformation phenomena : Twins, microbands, grain size effects, shear bands, and dynamic recrystallization. *J. Mater. Sci.*, 2004, **39**(4), 1153-1168.
  28. Hines, J.A.; Vecchio, K.S. & Ahzi, S. A model for microstructure evolution in adiabatic shear bands. *Metall. Mater. Trans. A*, 1998, **29**(1), 191-203.
  29. Xue, Q. & Gray, G.T. Development of adiabatic shear bands in annealed 316L stainless steel : Pt I. Correlation between evolving microstructure and mechanical behavior. *Metall. Mater. Trans. A*, 2006, **37**(8), 2435-2446.
  30. Xue, Q. & Gray, G.T. Development of adiabatic shear bands in annealed 316L stainless steel : Pt II. TEM studies of the evolution of microstructure during deformation localization. *Metall. Mater. Trans. A*, 2006, **37**(8), 2447-2458.
  31. Wang, X.B. Phenomenon of transformed adiabatic shear band surrounded by deformed adiabatic shear band of ductile metal. *Trans. Nonferr. Metal Soc.*, 2008, **18**(5), 1177-1183.
  32. Hu, C.J.; Lee, P.Y. & Chen, J.S. Ballistic performance and microstructure of modified rolled homogeneous armor steel. *J. Chinese Ins. Eng.*, 2002, **25**(1), 99-107.
  33. Bassim, M.N. & Odeshi, A.G. Shear strain localisation and fracture in high strength structural materials. *Arch. Mater. Sci. Eng.*, 2008, **31**(2), 69-74.
  34. Atapek, Ş.H. Formation of adiabatic shear bands in tempered steel under dynamic loading and their damage effects. *Mater. Test.*, 2012, **54**(9), 625-631.

#### Contributors



**Dr Ş. Hakan Atapek** received his MSc and PhD from Department of Metallurgical and Materials Engineering, Kocaeli University. He is working as Assistant Professor at Department of Metallurgical and Materials Engineering, Kocaeli University. He is also a postdoctoral researcher at Karlsruhe Institute of Technology, Institute für Angewandte Materialien-Werkstoffkunde.

His research area include: Physical metallurgy of steels, armor steels, materials characterization and fractography.